CFD simulation of thermal performances of building structure with expanded polystyrene (EPS) as thermal insulation

Milica Mirković, Zorana Petojević, Radovan Gospavić, Goran Todorović

Abstract—In this paper a three dimensional (3D), Computational Fluid Dynamics (CFD) simulation for indoor air flow and heat transfer in a single room was developed. The multi-layer structure building envelop, with expanded polystyrene (EPS) as thermal insulation inside, has been included into simulation and its influence on thermal performances were analysed. The indoor air flow and temperature distribution were analysed for different thicknesses of EPS insulations and were compared to the case without insulation. The commercial software FLUENT has been used in the simulation. The air flow due to natural convection is included into the model through a buoyancy-driven flow. The realizable k-ε model, based on Reynolds-Averaged Navier-Stokes (RANS) equations, is used for modelling of the turbulence in air flow. The radiator model with thermal flux as input parameter is used for simulation of heating of the room. In order to resolve flow in boundary layer high resolution grid near walls and low-Reynolds number has been used. According to the presented results the thickness of thermal insulation has significant influence on the indoor air flow and the temperature distribution inside the building.

Index terms — CFD simulation; building structure; temperature distribution, indoor air

I. INTRODUCTION

The significant part of global energy consumption goes to the energy use in buildings, mainly related to heating and cooling [1, 2]. Therefore, an improvement of the thermal performance and energy efficiency of the building structure would have a significant influence on the reduction in the energy consumption. The thickness of the insulation could be optimized by taking into account the requirements for the thermal performance of the building, energy costs and the initial cost of the insulation system [1-3]. The physical properties, geometry (thickness) of the insulation materials and geometry of building structure have significant influence on the thermal performance and energy efficiency of buildings. The most important parameters which influence the thermal performance of insulation materials are the thermal conductivity and the thickness of the

insulation material. The two main strategies for improvement of the thermal performance are use of new insulation materials with lower thermal conductivity or use of higher thickness of existing insulation materials [2]. The different numerical techniques and CFD simulations have been used for analysis of different aspects of heat transfer and air flow in different engineering applications including indoor and outdoor environments [4-10].

The interaction between indoor air and walls has important influence on air flow in the boundary layer and convective heat transfer coefficient (CHTC) [6]. The high resolution CFD simulations and low-Reynolds number modelling have been used for accurate estimation of CHTC for indoor CFD simulations [6]. A similar approach has been used to improve accuracy of CHTC on building facade for outdoor CFD simulations [7]. Another approach for assessment of the thermal performance of buildings is to use the coupled Building Energy and CFD [11, 12]. The approach uses the CHTC, which is obtained as output from the CFD calculation, as input parameter in the Building energy simulation [11]. To include the effect of the turbulence into the CFD simulations the various k-ε models have been used for indoor and outdoor airflow [6,7,13]. The main objective of the present study is to analyse the influence of EPS insulation thickness on thermal performance of a building structure by using a three dimensional CFD simulation for indoor air flow and heat transfer. The developed CFD simulation includes indoor air flow, indoor heat transfer in air and heat transfer through building envelope. The heating of the room has been simulated by the radiator model with thermal flux as input parameter. The CFD simulation is based on RANS [17-24] equations and the turbulence in air flow is taken into account by using *k-ε* model. The outdoor temperature has been considered as constant. The dimensions and the geometry of the building envelope have been included into the model. The building envelope is considered as a multi-layer structure. The natural convection due to heating has been modelled as buoyancy-driven flow. To improve the accuracy in CHTC modelling high resolution grid and low-Reynolds number has been used. To develop and perform CFD simulations the commercial software FLUENT has been used.

Milica Mirković is with the Faculty of Civil Engineering, Univesity in Belgrade, Bulevar Kralja Aleksandra 73, 11020 Belgrade, Serbia (e-mail: milicamirkovic91@ gmail.com).

Zorana Petojević is with the Faculty of Civil Engineering, Univesity in Belgrade, Bulevar Kralja Aleksandra 73, 11020 Belgrade, Serbia (e-mail: zjovanovic@ grf.bg.ac.rs).

Radovan Gospavić is with the Faculty of Civil Engineering, Univesity in Belgrade, Bulevar Kralja Aleksandra 73, 11020 Belgrade, Serbia (e-mail: rgospavic@ grf.bg.ac.rs).

Goran Todorović is with the Faculty of Civil Engineering, Univesity in Belgrade, Bulevar Kralja Aleksandra 73, 11020 Belgrade, Serbia (e-mail: todor@ grf.bg.ac.rs).

II. PHYSICAL MODEL OF TEMPERATURE FIELD AND AIR FLOW

The air flow has been modelled with Navier-Stokes (NS) equation. The standard form of the equation is given in the following form [14-16]:

$$\frac{\partial \vec{v}(\vec{r},t)}{\partial t} + (\vec{v}(\vec{r},t)\nabla)\vec{v}(\vec{r},t) = -\frac{1}{\rho}\nabla p(\vec{r},t) + \upsilon \cdot \Delta \vec{v}(\vec{r},t) + \vec{g}, \upsilon = \mu/\rho$$

$$(1)$$

where ρ [kg/m^2] is air density, $\vec{v}$ [m/s] is air velocity, p [Pa] is pressure, υ [m^2/s] is kinematic viscosity, μ [Pa·s] is air dynamic viscosity and g[m/s^2] is the gravitational acceleration. The first two terms on the left side of the equation (1) represent the total change of impulse of air per unit of volume, and the first term on the right side represents the change of impulse per unit of volume due to the pressure gradient, the second one is the contribution of the change of the impulse due to viscous friction between layers of fluid and the third one is due to the influence of gravitational acceleration. The principle of conservation of mass could be expressed by the equation of continuity:

$$\frac{\partial \rho}{\partial t} + \nabla(\rho \cdot \vec{v}) = 0 \qquad (2)$$

Fourier equation of heat conduction which includes convective heat transfer is given by the equation:

$$\rho c_p \left(\frac{\partial T}{\partial t} + \vec{v}\nabla T \right) = \nabla(\lambda \cdot \nabla T), \qquad (3)$$

where T [K] is temperature, c_p [J/kg K] is specific heat and λ [W/m·K] is coefficient of thermal conductivity. Convective heat transfer in the equation (3) is on the second member of the left. To close the system of equations (1-3), equation of state which connects the basic thermodynamic conditions, temperature, density and pressure should be given:

$$f(p,\rho,T) = 0. \qquad (4)$$

In our case, we will assume that the air is ideal gas. Pressure, temperature and density could be expressed as sum of mean values and perturbation terms in the following form:

$$p = p_0 + \delta p, \ T = T_0 + \delta T, \ \rho = \rho_0 + \delta \rho = \rho_0 - \beta \rho_0 \delta T,$$
$$p_0 = \rho_0 \cdot \vec{g} \cdot \vec{r} \qquad (5)$$

where δp, δT and $\delta \rho$ are the perturbations in pressure, temperature and density respectively, while p_0, T_0 and ρ_0 are pressure, temperature and density in thermal equilibrium, β [1/K] is the thermal expansion coefficient. By using the expressions for small perturbations in relations (1-4), the following expressions for buoyancy-driven flow could be obtained:

$$\frac{\partial \vec{v}}{\partial t} + (\vec{v} \cdot \nabla)\vec{v} = -\frac{1}{\rho_0}\nabla \delta p - \beta \cdot \delta T \cdot \vec{g} + \upsilon \cdot \Delta \vec{v}, \ \nabla \vec{v} = 0,$$

$$\frac{\partial \delta T}{\partial t} + \vec{v} \cdot \nabla \delta T = \nabla(\lambda \cdot \nabla \delta T). \qquad (6)$$

The effect of turbulence is included using the Reynolds averaging formulation (RANS). According to this approach the velocity and pressure are split into main value and the fluctuation part, where the mean value is obtained by averaging over ensemble.

As a result of averaging there are two additional dynamic size: k [m^2/s^2] is averaged turbulent kinetic energy and ε [m^2/s^3] is velocity of dissipation. The propagation of turbulent kinetic energy and its dissipation within the fluid with two additional transport equations for k and ε have been provided. In this way, the system of equations has been closed because the number of unknowns (dynamic size: $p, v_x, v_y, v_z, T, k, \varepsilon$) is equal to the number of equations. This model of turbulence is called RANS formulation.

III. CFD SIMULATION

Three dimensional (3D) indoor airflow and heat transfer in a single room during heating have been analysed using CFD simulation. The room with one door and two windows, which has two interior and two outside walls, ceiling and floor, is considered. The heating of the room has been considered by radiator model with heat flux as an input parameter. The geometry of the room with dimensions and positions of windows, door and radiator are presented in Fig. 1. Temperatures T_{out} and T_{in} indicate in Fig. 1 the outdoor and indoor temperature, respectively, which have been used as boundary conditions on the walls, windows and door. The dimensions of the room are L×B×H = 5×4×2,53 m^3, and other dimensions from figure 1a are a = 0,4 m, c = 1,63 m. Internal wall surfaces which belong to the building envelope are labelled *wall 3* and *wall 4* while surfaces on the internal walls are labelled *wall 1* and *wall 2*, as indicate in Fig.1. The dimensions of the door are 0,95 (width) × 2,06 (height) m^2 and the dimensions of the windows (Fig. 1 and 2) are B_W (width) × H_W (height) = 1,4 × 1,53 m^2. The radiator is placed below the windows and its position and other dimensions in vertical x-z plane are shown in Fig. 2, where d_{rad} = 0,1 m and H_1 = 0,32 m. The dimensions of the radiator are 3,2 (length) × 0,53 (height) m^2. It has been assumed that the thermal flux from the radiator is constant and equal to 500 W/m^2 in all simulations. The coordinate origin is placed on the floor of the room and its position in x-y plane is indicated in Fig. 1. The building envelope consists of four layers: inside layer of mortar, concrete, insulation and brick. Detailed dimensions, structure and material properties of building envelope are presented in Table 1 [28]. Air indoor flow and heat transfer for three thicknesses (2,5; 5 and 10 cm) of EPS insulation inside the building envelope are analysed. The case without thermal insulation is analysed as well and compared to the case with insulation. The structure, thermal parameters and thicknesses of the internal walls, door and windows are presented in Tables 2 and 3. The windows are considered to have double glazing. Equivalent values for density ρ_{eq}, specific heat c_{peq} and thermal conductivity λ_{eq} are calculated using following relations:

$$\rho_{eq} = \frac{\sum_{i=1}^{N} d_i \cdot \rho_i}{\sum_{i=1}^{N} d_i}; \quad c_{peq} = \frac{\sum_{i=1}^{N} d_i \cdot \rho_i \cdot c_{pi}}{\sum_{i=1}^{N} d_i \cdot \rho_i}; \quad \lambda_{eq} = \frac{\sum_{i=1}^{N} d_i}{\sum_{i=1}^{N} \frac{d_i}{\lambda_i}}, \quad (7)$$

where N is the number of layers and d_i is the thickness of ith layer. The floor, ceiling, internal walls and windows are modelled as thermal resistances R_T =d/λ_{ek}, where *d* [m] is the thickness of the considered structure and λ [W/(m·K)] is the equivalent thermal conductivity. A structured hexahedral grid with 338,800 cells inside the indoor space has been used. The spatial resolution in the central part of the domain is 10 cm, while the resolution in the boundary layer next to the walls is 1mm. The same type of grid has been used in

the building envelop. The size of the grid for the building envelope was 33,848 and 25,221 cells for cases with and without insulation respectively. To improve the accuracy in CHTC modelling a high resolution grid and a low-Reynolds number modelling have been used [7]. The grid and computational domain with the coordinate system are shown in Fig. 3.

The insulation thickness for the case shown in this figure is equal to 8 cm. No-slip boundary conditions have been used for air flow on walls. For the sake of simplicity the outside temperature T_{out} (Fig 1.) and the heat transfer coefficient on the outside surface of the building envelop, h_{out}, are assumed to be constant and equal to -18°C and 18 [W/(m^2·K)] respectively [25,7]. The indoor air temperature in rooms next, above and below the considered room, T_{in}, (Fig 1.) and convective heat transfer coefficients on wall surfaces in these rooms, h_{in}, are assumed to be constant and equal to 20°C and 8 [W/(m^2·K)], respectively [25]. The following convective boundary conditions for equation (3) on the outer surface of building envelope (subscript "out"), interior walls, door, ceiling and floor (subscript "in") are used:

$$-\lambda \frac{\partial T_w}{\partial n} = h_{out/in} \cdot \left(T_w - T_{out/in}\right), \qquad (8)$$

where T_w is corresponding surface temperature. It has been assumed that construction layers inside the building envelope are in ideal thermal contact. Adiabatic wall boundary condition has been used for the top and bottom surfaces of the building envelope (Fig. 2.). The simulation has been carried out by performing a large number of time iterations (more than 30000 time iterations) until no considerable change in temperature distribution has been observed (less than 1% for relative temperature variations has been adopted as threshold value). The radiator has been considered as infinitely thin surface and it is modelled using the following relations [27]:

$$q_{rad} = q_{down} - q_{up}; \quad q_{rad} = h_{rad} \cdot \left(T_{rad} - T_{up}\right), \qquad (9)$$

where q_{rad} [W/m^2] and T_{rad} [K] are the thermal flux and temperature on the radiator surface, respectively, $T_{up/down}$ [K] are the upstream and downstream air temperatures respectively, h_{rad} [W/(m^2 ·K)] is the heat transfer coefficient for the radiator and $q_{up/down}$ [W/m^2] are the upstream and downstream thermal fluxes in the normal direction to the radiator surface. The pressure loss Δp [Pa] through the radiator is modelled by using the following relation:

$$\Delta p = k_{loss} \cdot \frac{1}{2} \cdot \rho \cdot v_n^2, \qquad (10)$$

where k_{loss} is non-dimensional loss-coefficient which could be specified as an empirical constant or function of normal air velocity through the radiator. In this study the following constant values related to the radiator model are assumed: q_{rad} = 500 W/m^2; k_{loss} = 350 ; h_{rad} =6,523 W/(m^2·K). A pressure based solver is used and a pressure-velocity coupling is obtained by the SIMPLE algorithm. The body force weighted spatial discretization for pressure is utilized. A second order upwind spatial discretization is used for the energy, convection and viscous terms in the governing equation. A second order implicit time discretization with fixed time step equal to 0,1 – 0,5 sec was used.

Table 1. Dimensions and physical parameters of materials used in the building envelope.

	Material	ρ [kg/m^2]	c_p [J/(kg·K)]	λ [W/m·K]	d [cm]	wall d [cm]
1	mortar	1800	1050	0.87	2.0	36.5; 39.0; 44.0
2	concrete	2500	960	2.33	20.0	
3	insulation EPS	20	1.26	0.041	2.5 ; 5; 10	
4	brick	1600	920	0.64	12	

Table 2. Structure, dimensions, thermal parameters and equivalent values for the floor and ceiling

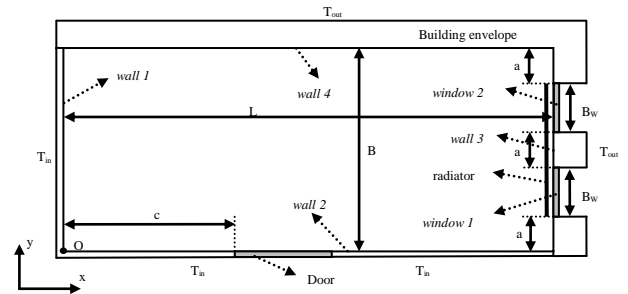| Building structure	Material	ρ [kg/m^2]	c_p [J/(kg·K)]	λ [W/m·K]	d [cm]
floor and ceiling	wood (parquet)	700	1670	0.21	2.5
	screed	2200	1050	1.4	4.0
	extruded polystyrene	33	1500	0.035	2.0
	concrete	2500	960	2.33	20.0
	mortar	1800	1050	0.87	2.0
	Eqv. value	2105.4	997.28	0.37	30.5

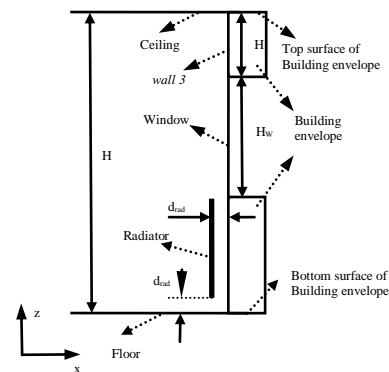Fig. 1. Schematic view of the room in the x-y plane

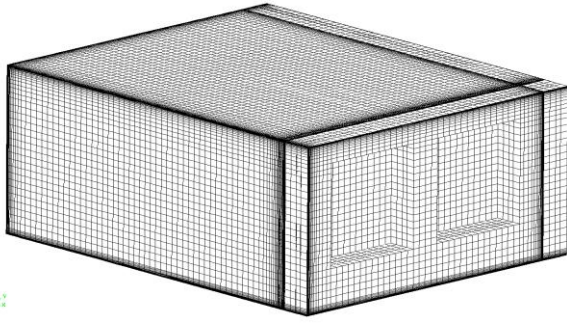Fig. 2. Schematic view of the room in the x-z plane

Fig. 3. Grid and computational domain with the coordinate system.

Table 3. Structure, dimensions, thermal parameters and equivalent values for the internal walls, door and windows.

Building structure	Material	ρ [kg/m²]	c_p [J/(kg·K)]	λ [W/m·K]	d [cm]
internal walls	gypsum	1400	840	0.7	7.0
door	wood	546	2720	0.15	5.0
windows double glassing	glass × 2 layers	2800	700	0.8145	0.25
	air	1.205	1005	0.0257	0.5
	Eqv. value	1400.6	770.101	0.0498	1.0

IV. RESULTS AND DISCUSSION

To analyse the thermal performances of EPS, a CFD simulation has been carried out. Four different thicknesses of EPS insulation layer inside the building envelope are considered: 0, 2,5, 5 and 10 cm. In these simulations only the thickness of the insulation material has been changed while the other model parameters have been kept constant. The positions of the internal surfaces which are labelled as *wall 1-4* are shown in Fig.1. All distances are measured from the coordinate origin O which position is indicated in Fig. 1. The temperatures and velocities in all figures are expressed in [°C] and [m/s], respectively.

Comparisons between temperature distributions in the indoor air for different thicknesses of the insulation material are presented in Fig. 4.
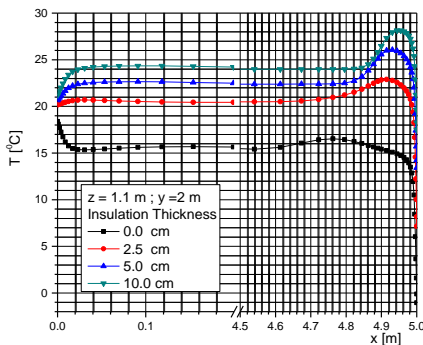

Fig. 4. Comparison between the temperature distributions in the indoor air for four thicknesses of the insulation material (EPS): 0; 2.5; 5 and 10 cm, in the x- direction, along line which is 1.1 m above floor and 2 m from wall 2

The temperature distributions are obtained in the x-direction, 1.1 m above the floor, along three different lines which are at a distance of 2 m from *wall 2* (middle of the room) from *wall 4*. From the results presented in Fig. 4, one can see that the air temperature rises near the wall 3 surface (x=5m) for all EPS thicknesses due to heat realised from radiator and consequent hot air flow. Flow field near the wall 3 consists of two streams, hotter air flowing upward and colder flowing downward which is in contact to the wall surface. Also, as the EPS thickness grows the hotter air stream shrinks and get closer to the wall. Along with this there are decrease in width of convective heat transfer region. It could be concluded that the thickness of the insulation material has great influence on the indoor air flow and thermal performance of the building envelope.

The comparison between the temperature distributions inside the building envelope along same directions as in the previous case is presented in Fig. 5.
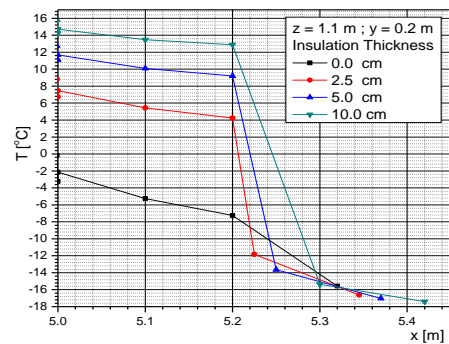

Fig. 5. Comparison between temperature distributions inside the building envelope for different thicknesses of the insulation material (EPS) in the x- direction, along a line which is 1.1 m above floor and 0.2 m from wall 2

Temperature difference in the middle of the room (x=2,5 m ; y=2m) at the height of 1.1 m from the floor between the case with the thickness thermal insulation (10 cm) and the case without thermal insulation is more than 9°C.

From Fig. 5 could be seen that the temperature inside the building envelope for the case without insulation is below zero. This could have a significant influence on the hygrothermal performance of the building envelope [6, 26]. The temperature in the concrete of the wall is considerably higher and above 0 °C for all the cases with thermal insulation.
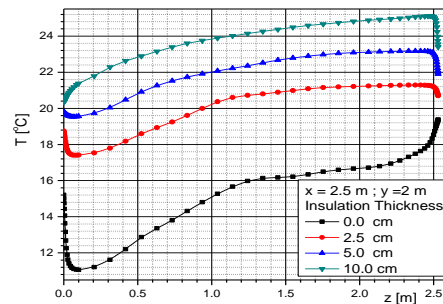

Fig. 6. Comparison between the four temperature distributions of indoor air for different insulation materials thicknesses of EPS in the vertical direction, along a vertical line placed 2m from *wall 2* and 2,5m from the *wall 1*.

From Fig. 6 could be seen that the air temperature near the floor for the case without thermal insulation is more than 7°C lower than for the case with 10cm of insulation. The behaviour of the temperature profile near the walls depends on the insulation thickness as well. For the cases with 2,5cm and without insulation the surface temperature of the floor is higher than the air temperature near the floor. It could be noticed that a very thick layer of cold air, which is on temperature lower than the surface temperature of the floor, is trapped near the floor for the case without insulation. The thickness of this layer reaches 1m at the middle of the room (Fig. 6). The temperature distribution in the y-direction, 10 cm from *wall 3* (wall with windows and radiator) at a distance of: 0,1m from the floor, and 0,1m from the ceiling are presented in Fig. 7, respectively.
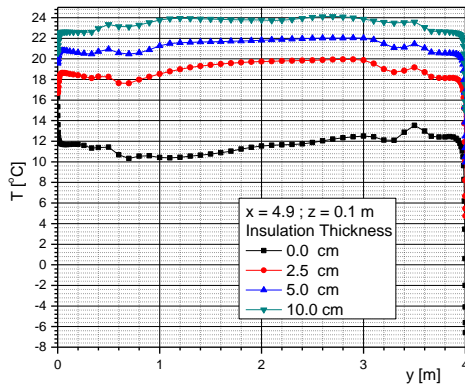

Fig. 7. Temperature distribution for different thicknesses of the insulation material in the y-direction, 0.1 m from the *wall 3* and 0.1 from floor

In Fig. 8 the velocity field in the vertical plane parallel to the x-direction which is at a distance of 2m from *wall 2* are presented. The thicknesses of the insulation material corresponding to results presented in Fig. 8 are equal to 2,5cm.
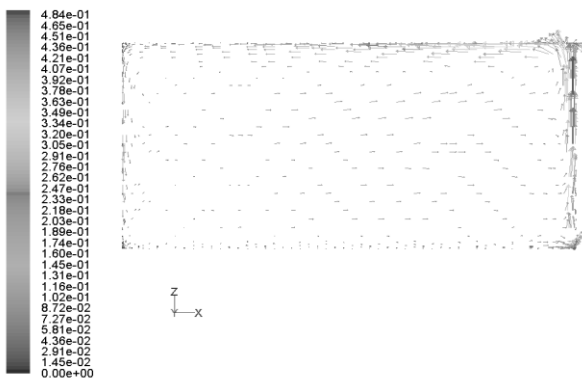

Fig. 8. The velocity field in the vertical plane which contains the radiator and which is 0,1 m from the *wall 3*; velocities are expressed in [m/s].Thicknesses of thermal insulation is: 2,5 cm

From these results it can be seen that the insulation thickness has a significant influence on the air flow in the vertical plane parallel to the x-direction in the middle of the room, not only in the space near radiator but also in the air layer near the ceiling. For thicker insulation (10 cm) the

maximal air velocities in the vertical direction near the radiator and in the horizontal direction near the ceiling are around 0.48 m/s and 0.35 m/s, respectively. For the case when the insulation thickness is 2,5 cm the maximal air velocities in the vertical and horizontal directions are 0,337 m/s and 0,2 m/s, respectively. From these results it follows that the maximal air velocity in the vertical and horizontal directions in this plane will increase approximately for 42% and 75%, respectively, when EPS insulation thickness is increased from 2,5 cm to 10 cm. From this analysis it could be concluded that the temperature distribution in the whole volume of the room will be more homogeneous for the cases with thicker thermal insulation.

V. CONCLUSIONS

The 3D CFD simulation for the indoor air flow and heat transfer was developed. The k-ε RANS model has been used to take into account the effect of turbulence in air flow. The heating of the room has been simulated using the radiator model. The thermal performance of the building envelope with different thicknesses of the EPS insulation layer was analysed. It is assumed that the outside temperature was constant and equal to -18 °C. Three cases with different insulation thicknesses: 2,5; 5 and 10 cm, as well as without insulation, were considered. The temperature distribution inside air and building walls for different thicknesses of the EPS insulation were analysed. It has been obtained that insulation thickness has a significant influence on the temperature distribution and the air flow. It is obtained that the temperature in the middle of the room at the height of 1,1 m from the floor for the case with insulation thickness of 10 cm is 9 °C higher than for the case without insulation. The temperature distribution inside the building envelope was analysed as well. It was obtained that the temperature inside the building walls for the case without insulation is below zero, which could have detrimental influence on the hygrothermal behaviour of the building envelope. The numerical results for the air velocity in the vertical planes parallel to the x and y directions were analysed. It has been obtained that the maximal air velocity in the vertical and horizontal directions, in the vertical plane which is in the middle of the room and parallel to the x direction, will increase approximately for 42% and 75%, respectively, when EPS insulation thickness is increased from 2,5 cm to 10 cm.

REFERENCES

[1] Omer Kaynakli, A review of the economical and optimum thermal insulation thickness for building applications, Renewable and Sustainable Energy Reviews. **16**, 415-425 (2012). DOI:10.1016/j.rser.2011.08.006

[2] Bjørn Petter Jelle, Traditional, state-of-the-art and future thermal building insulation materials and solutions - Properties, requirements and possibilities, Energy and Buildings. **43**, 2549-2563 (2011). DOI:10.1016/j.enbuild.2011.05.015

[3] McKinsey, Pathways to a Low-Carbon Economy, Version 2 of the Global Greenhouse Gas Abatement Cost Curve, McKinsey & Company, 2009.

[4] Sami A. Al-Sanea, M.F. Zedan, M.B. Al-Harbi, Heat transfer characteristics in air-conditioned rooms using mixing air-distribution system under mixed convection conditions, International Journal of

[6] H.J. Steeman, A.Janssens, J.Carmeliet, M.DePaepe, Modelling indoor air and hygrothermal wall interaction in building simulation: Comparison between CFD and a well-mixed zonal model, Building and Environment. **44**, 572-583 (2009). DOI: 10.1016/j.buildenv.2008.05.002

[7] B. Blocken, T. Defraeye, D. Derome, J. Carmeliet, High-resolution CFD simulations for forced convective heat transfer coefficients at the facade of a low-rise building, Building and Environment. **44**, 2396-2412 (2009). DOI:10.1016/j.buildenv.2009.04.004

[8] Radovan Gospavić, Björn Margeirsson, Viktor Popov, Mathematical model for estimation of the three-dimensional unsteady temperature variation in chilled packaging units, International Journal of Refrigeration, **35**, 1304-1317 (2012) DOI:10.1016/j.ijrefrig.2012.04.002

[9] Björn Margeirsson, Radovan Gospavić, Halldór Pálsson, Sigurjón Arason, Viktor Popov, Experimental and numerical modelling comparison of thermal performance of expanded polystyrene and corrugated plastic packaging for fresh fish, International Journal of Refrigeration, **34**, 573-585 (2011) DOI:10.1016/j.ijrefrig.2010.09.017

[10] A. Kovačević, M. Srećković, R. Gospavić, S. Ristić, P. Jovanić, Laser-PMMA Interaction and Mechanical Stresses, ACTA PHYSICA POLONOCA A. **112**, 981-986 (2007)

[11] Zhiqiang John Zhaia, Qingyan Yan Chenb, Performance of coupled building energy and CFD simulations, Energy and Buildings. **37**, 333-344 (2005). DOI:10.1016/j.enbuild.2004.07.001

[12] M. Bartaka, I. Beausoleil-Morrisonb, J.A. Clarkec, J. Denevd, F. Drkala, M. Laina, I.A. Macdonaldc, A. Melikove, Z. Popiolekf, P. Stankovd, Integrating CFD and building simulation, Building and Environment. **37**, 865-871 (2002).

[13] Jiantao Shao, Jing Liu, Jianing Zhao, Evaluation of various non-linear k-ε models for predicting wind flow around an isolated high-rise building within the surface boundary layer, Building and Environment. **57**, 145-155 (2012). DOI:10.1016/j.buildenv.2012.04.018

[14] Landau and Lifshitz, Course of Theoretical Physics Volume 6, Fluid Mechanics, second ed., Pergamon Press, Oxford, New York, 1993.

Thermal Sciences. **59**, 247-259 (2012). DOI: 10.1016/j.ijthermalsci.2012.04.023

[5] M. Salmanzadeh, Gh.Zahedi, G.Ahmadi, D.R.Marr, M.Glauser, Computational modelling of effects of thermal plume adjacent to the body on the indoor airflow and particle transport, Journal of Aerosol Science. **53**, 29-39 (2012). DOI: 10.1016/j.jaerosci.2012.05.005

[15] W. Michael Lai, David Rubin, Erhart Krempl: Introduction to Continuum Mechanics, fourth ed., Butterworth-Heinemann Ltd, Oxford, 1993.

[16] A. Pantokratoras, Effect of viscous dissipation in natural convection along a heated vertical plate, Applied Mathematical Modelling. **29**, 553–564 (2005). DOI:10.1016/j.apm.2004.10.007

[17] Jean Mathieu, Julian Scott, An Introduction to Turbulent Flow, first ed., Cambridge University Press, Cambridge, New York, 2000.

[18] Hineze J O, Turbulence, second ed., McGrow-Hill Publishing Co. New York, 1975.

[19] M.M. Stanisic, The Mathematical Theory of Turbulence, second ed., Springer-Verlag, New York, 1988.

[20] N.G. Wright , G.J. Easom, Non-linear k–e turbulence model results for flow over a building at full-scale, Applied Mathematical Modelling. **27**, 1013–1033 (2003). DOI:10.1016/S0307-904X(03)00123-9

[21] Sowjanya Vijiapurapu, Jie Cui, Performance of turbulence models for flows through rough pipes, Applied Mathematical Modelling. **34**, 1458–1466 (2010). DOI:10.1016/j.apm.2009.08.029

[22] P. Gardin , M. Brunet , J.F. Domgin , K. Pericleous , An experimental and numerical CFD study of turbulence in a tundish container, Applied Mathematical Modelling. **26**, 323–336 (2002).

[23] Launder BE, Spalding DB, The numerical computation of turbulent flows, Computer Methods in Applied Mechanics and Engineering. **3**, 269-89 (1974).

[24] M.L. Hoang, P. Verboven, J. De Baerdemaeker, B.M. Nicola, Analysis of the air in a cold store by means of computational fluid dynamics, International Journal of Refrigeration. **23**, 127-140 (2000).

[25] Hartwig M. Künzel, Simultaneous Heat and Moisture Transport in Building Components, one and two dimensional calculation using simple parameters, PhD thesis, Fraunhofer Institute of Building Physics, Fraunhofer IRB Verlag Suttgard 1995.

[26] Jan Toman, Alena Vimmrova , Robert Cerny , Long-term on-site assessment of hygrothermal performance of interior thermal insulation system without water vapour barrier, Energy and Buildings. **41**, 51–55 (2009).